

Topological superconductivity in Janus monolayer transition metal dichalcogenides

Xian-Dong Li(李现东), Zuo-Dong Yu(余作东), Wei-Peng Chen(陈伟鹏), and Chang-De Gong(龚昌德)

Citation: Chin. Phys. B, 2022, 31 (**11**): 110304. DOI: 10.1088/1674-1056/ac8739

What follows is a list of articles you may be interested in

Spin-orbit coupling adjusting topological superfluid of mass-imbalanced Fermi gas

Jian Feng(冯鉴), Wei-Wei Zhang(张伟伟), Liang-Wei Lin(林良伟), Qi-Peng Cai(蔡启鹏), Yi-Cai Zhang(张义财), Sheng-Can Ma(马胜灿), and Chao-Fei Liu(刘超飞)

Chin. Phys. B, 2022, 31 (**9**): 090305. DOI: 10.1088/1674-1056/ac6860

Hard-core Hall tube in superconducting circuits

Xin Guan(关欣), Gang Chen(陈刚), Jing Pan(潘婧), and Zhi-Guo Gui(桂志国)

Chin. Phys. B, 2022, 31 (**8**): 080302. DOI: 10.1088/1674-1056/ac633b

Exploring Majorana zero modes in iron-based superconductors

Geng Li(李更), Shiyu Zhu(朱诗雨), Peng Fan(范朋), Lu Cao(曹路), and Hong-Jun Gao(高鸿钧)

Chin. Phys. B, 2022, 31 (**8**): 080301. DOI: 10.1088/1674-1056/ac70c3

Topological phase transition in cavity optomechanical system with periodical modulation

Zhi-Xu Zhang(张志旭), Lu Qi(祁鲁), Wen-Xue Cui(崔文学), Shou Zhang(张寿), and Hong-Fu Wang(王洪福)

Chin. Phys. B, 2022, 31 (**7**): 070301. DOI: 10.1088/1674-1056/ac4a6a

Beating standard quantum limit via two-axis magnetic susceptibility measurement

Zheng-An Wang(王正安), Yi Peng(彭益), Dapeng Yu(俞大鹏), and Heng Fan(范桁)

Chin. Phys. B, 2022, 31 (**4**): 040309. DOI: 10.1088/1674-1056/ac4229

Topological superconductivity in Janus monolayer transition metal dichalcogenides

Xian-Dong Li(李现东)[1], Zuo-Dong Yu(余作东)[1,2,†], Wei-Peng Chen(陈伟鹏)[3,‡], and Chang-De Gong(龚昌德)[1,4,5]

[1] *National Laboratory of Solid State Microstructure, Department of Physics, Nanjing University, Nanjing* 210093, *China*
[2] *School of Information and Electronic Engineering, Zhejiang Gongshang University, Hangzhou* 310018, *China*
[3] *Shenzhen Institute for Quantum Science and Engineering, Southern University of Science and Technology, Shenzhen* 518055, *China*
[4] *Center for Statistical and Theoretical Condensed Matter Physics, Zhejiang Normal University, Jinhua* 321004, *China*
[5] *Collaborative Innovation Center of Advanced Microstructures, Nanjing University, Nanjing* 210093, *China*

(Received 8 June 2022; revised manuscript received 19 July 2022; accepted manuscript online 5 August 2022)

The Janus monolayer transition metal dichalcogenides (TMDs) MXY (M = Mo, W, *etc*. and X,Y = S, Se, *etc*.) have been successfully synthesized in recent years. The Rashba spin splitting in these compounds arises due to the breaking of out-of-plane mirror symmetry. Here we study the pairing symmetry of superconducting Janus monolayer TMDs within the weak-coupling framework near critical temperature T_c, of which the Fermi surface (FS) sheets centered around both Γ and K (K') points. We find that the strong Rashba splitting produces two kinds of topological superconducting states which differ from that in its parent compounds. More specifically, at relatively high chemical potentials, we obtain a time-reversal invariant $s+f+p$-wave mixed superconducting state, which is fully gapped and topologically nontrivial, *i.e*., a $\mathbb{Z}_2$ topological state. On the other hand, a time-reversal symmetry breaking $d+p+f$-wave superconducting state appears at lower chemical potentials. This state possess a large Chern number $|C|=6$ at appropriate pairing strength, demonstrating its nontrivial band topology. Our results suggest the Janus monolayer TMDs to be a promising candidate for the intrinsic helical and chiral topological superconductors.

Keywords: topological, superconductivity, Janus, transition metal dichalcogenides (TMDs)

PACS: 03.65.Vf, 74.20.Rp, 74.25.Dw, 82.45.Mp **DOI:** 10.1088/1674-1056/ac8739

1. Introduction

Topological superconductors (TSCs), which are characterized by a full-gap bulk and robust gapless surface (edge) states, have gained much attention for their novel topological properties in recent years.[1–9] Several superconductors are considered to be unconventional and even topologically nontrivial, including Sr_2RuO_4[10–13] and heavy fermion compounds.[14–16] There are also theoretical proposals for artificially realizing the topological superconducting states by using the s-wave superconductor together with spin–orbit coupling (SOC). For instance, through the proximity effect an s-wave superconductor on a strong topological insulator becomes a spinless $p+\mathrm{i}p$-wave superconductor[1] or by applying a strong perpendicular magnetic field to an s-wave Rashba superconductor, topological superconducting states emerge.[17,18] However, there has been no definitive experimental evidence for the existence of TSCs so far, and it is still a grand challenge to provide valuable traces of them.

Transition metal dichalcogenides (TMDs) are a class of noncentrosymmetric layered van der Waals materials, which have been studied for decades as they usually exhibit superconductivity, charge-density wave state and other electronic phenomena.[19–24] Superconductivity in the bulk TMDs is usually conventional. However, in the ultra-thin films, a strong enhancement of the in-plane critical field indicates possible unconventional superconductivity caused by the large Ising SOC.[25–30] Several kinds of parity-mixed pairings, for instance, the $s+f$-wave and $d+p$-wave pairings, have been suggested as candidates for unconventional superconducting states in the monolayer TMDs.[31,33]

Here we study the pairing symmetry of the newly synthesized Janus TMDs MXY.[33–40] In a Janus TMD molecular layer, M atomic plane is sandwiched by two different atomic planes X and Y. The stacking structure breaks the out-of-plane mirror symmetry, leading to a Rashba-type spin splitting of bands around Γ point in the Brillouin zone (BZ). Previous works on the Janus layered TMDs mainly focused on their crystal, band structures and optical property,[41–44] while the nature of possible superconductivity has rarely been discussed. The parents of Janus TMDs, which have the 2H structure, are intrinsic Ising superconductors in most thin layer cases. We focus on the Janus TMDs with FS sheets centered around both Γ and K (K') points based on the observation that the Rashba spin splitting occurs around Γ[36] while the Ising-type acts mainly on the K (K') valleys.[45] The Cooper pairs are thus subjected to these two kinds of SOC effects. This type of FS topology provides an ideal platform for us to investigate the competition and interplay between these SOC effects on superconductivity. Naturally one could expect that the Rashba–

†Corresponding author. E-mail: richzyu@gmail.com
‡Corresponding author. E-mail: chenwp@sustech.edu.cn

© 2022 Chinese Physical Society and IOP Publishing Ltd

Ising superconductivity leads to various kinds of mixed superconducting states in the Janus monolayer TMDs. As far as we know, the superconducting symmetry of H–MoS_2 monolayer coexisting with a gating-induced Rashba SOC has been theoretically studied by Yuan *et al.* in Ref. [31]. But since the FS of MoS_2 encloses only at K (K') points, we believe the influence of Rashba SOC on Ising superconductivity is still not completely revealed.

In this work, we calculate the most favorable pairing states of the Janus monolayer with both Γ and K (K') centered FS at different pairing interactions and chemical potentials by solving the linearized gap equation near the critical temperature T_c. We obtain a rich phase diagram which shows that at a relatively high chemical potential, a time-reversal invariant (TRI) $s+f+p$-wave pairing in irreducible representation (IR) A_1 of point group C_{3v} may dominate the nearest-neighbor (NN) pairing channels. Unlike the nodal $s+f$-wave pairing in the monolayer H–MX_2,[46] the $s+f+p$-wave has a large additional helical p-wave component induced by the strong Rashba SOC, making the superconductor to be full-gap and topologically nontrivial, characterized by the invariant $\mathbb{Z}_2=1$. At a lower chemical potential, a time-reversal symmetry breaking (TRB) $d+p+f$-wave pairing belonging to the two-dimensional IR E appears, which can be a large-Chern-number chiral superconducting state with Chern number $|C|=6$ at appropriate pairing strengths. We emphasis that in the absence of Rashba SOC, a TRB $d+p$-wave pairing obtained from the same type of FS geometry always lead to a topologically trivial state, *i.e.*, $C=0$.

2. Model

The crystal structure of the Janus monolayer TMD is shown in Fig. 1(a). It can be viewed as a monolayer H–MX_2 whose top-layer X atoms are replaced by another Y atoms, which breaks the out-of-plane mirror symmetry. The normal-state tight-binding Hamiltonian is constructed as follows:

$$h_{0,\boldsymbol{k}} = \xi_{\boldsymbol{k}} + (\boldsymbol{\alpha}_{\boldsymbol{k}} + \boldsymbol{\beta}_{\boldsymbol{k}})\cdot\boldsymbol{\sigma}, \tag{1}$$

$$\xi_{\boldsymbol{k}} = \sum_{j=1}^{3}[-2t\cos k_j - 2t_1\cos(k_j - k_{j+1})] - \mu, \tag{2}$$

$$\boldsymbol{\alpha}_{\boldsymbol{k}} = \alpha_R\left\{\frac{\sqrt{3}}{2}\boldsymbol{x}(\sin k_2 - \sin k_3) - \boldsymbol{y}\left[\sin k_1 - \frac{1}{2}(\sin k_2 + \sin k_3)\right]\right\}, \tag{3}$$

$$\boldsymbol{\beta}_{\boldsymbol{k}} = \beta_{\rm so}\boldsymbol{z}(\sin k_1 + \sin k_2 + \sin k_3), \tag{4}$$

where $k_j = \boldsymbol{k}\cdot\boldsymbol{R}_j$, with bond vectors $\boldsymbol{R}_1 = a\boldsymbol{x}$,

$$\boldsymbol{R}_2 = a\left(-\frac{1}{2}\boldsymbol{x} + \frac{\sqrt{3}}{2}\boldsymbol{y}\right),\quad \boldsymbol{R}_3 = a\left(-\frac{1}{2}\boldsymbol{x} - \frac{\sqrt{3}}{2}\boldsymbol{y}\right),$$

and $\boldsymbol{R}_4 \equiv \boldsymbol{R}_1$. a is the lattice constant, μ is the chemical potential, and t and t_1 denote the NN and next NN hoppings, respectively. $\boldsymbol{\alpha}_{\boldsymbol{k}}$ and $\boldsymbol{\beta}_{\boldsymbol{k}}$ are effective magnetic fields caused by Rashba and Ising SOC with $\alpha_{\rm R}$ and $\beta_{\rm so}$ representing corresponding strengths, respectively. We choose the value of parameters to be $(t, t_1, \alpha_{\rm R}, \beta_{\rm so}) = (-0.06, -0.14, 0.032, 0.067)$ eV. The choice of $\alpha_{\rm R}$ is referred to MXY (M = W, Mo and X, Y = S, Se, Te) in Ref. [36], whose Rashba splitting strength ranges from 77 meV·Å to 518 meV·Å, corresponding to $\alpha_{\rm R}$ value ranging from 0.015 eV to 0.10 eV in our lattice model by assuming the lattice constant $a = 3.3$ Å.[45]

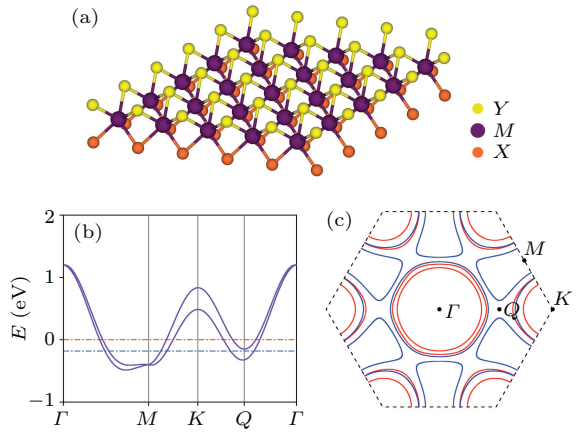


Fig. 1. (a) Crystal structure of a Janus monolayer H–MXY. (b) The constructed band structure of it. Fermi levels at $\mu = 0$ eV and -0.18 eV are denoted by the red and blue dashed lines, respectively, and their corresponding FS in the first Brillouin zone are presented in panel (c).

We set the chemical potential μ as an tunable parameter in our model. When $\mu = 0$ eV, this model is in analogy to the band structure of H–TaS_2 given by experiments and DFT calculations.[45,47,48] On the other hand, a chemical potential $\mu = -0.18$ eV will give an FS topology similar to H–$TaSe_2$, which has dog-bone-shaped electron Fermi pockets centered at M.[49–51] The low-energy spectrum and FS of H–MXY for the two chemical potentials, $\mu = 0$ eV and -0.18 eV, are simulated in Figs. 1(b) and 1(c). In the figure of BZ, the "Q" point labels the position of van Hove singularity (vHS) corresponding to the first Lifshitz transition. One can infer from the figure that the first Lifshitz transition occurs around $\mu = -0.15$ eV.

Table 1. The classification of basis gap functions based on C_{3v} symmetry. They are introduced as: $C(\boldsymbol{k}) = (1/\sqrt{3})\sum_{i=1}^{3}\cos k_i$, $C_+(\boldsymbol{k}) = (1/\sqrt{3})\sum_{i=1}^{3}\omega^{i-1}\cos k_i$, $S(\boldsymbol{k}) = (1/\sqrt{3})\sum_{i=1}^{3}\sin k_i$, $S_+(\boldsymbol{k}) = (1/\sqrt{3})\sum_{i=1}^{3}\omega^{i-1}\sin k_i$, $C_-(\boldsymbol{k}) = C_+^*(\boldsymbol{k})$, $S_-(\boldsymbol{k}) = S_+^*(\boldsymbol{k})$, with vector $\boldsymbol{x}_\pm = (\boldsymbol{x} \pm \mathrm{i}\boldsymbol{y})/2$ and phase factor $\omega = \exp(-\mathrm{i}2\pi/3)$.

Γ	Singlet	Triplet
A_1	$\Psi^{A_1,on} = 1/\sqrt{2}$ $\Psi^{A_1,nn} = C(\boldsymbol{k})$	$\boldsymbol{d}^{A_1,z} = S(\boldsymbol{k})\boldsymbol{z}$ $\boldsymbol{d}^{A_1,xy} = \mathrm{i}[S_-(\boldsymbol{k})\boldsymbol{x}_+ - S_+(\boldsymbol{k})\boldsymbol{x}_-]$
A_2		$\boldsymbol{d}^{A_2,xy} = S_-(\boldsymbol{k})\boldsymbol{x}_+ + S_+(\boldsymbol{k})\boldsymbol{x}_-$
E	$\begin{cases}\Psi_1^{E,nn} = C_+(\boldsymbol{k})\\ \Psi_2^{E,nn} = C_-(\boldsymbol{k})\end{cases}$	$\begin{cases}\boldsymbol{d}_1^{E,z} = S_+(\boldsymbol{k})\boldsymbol{z}\\ \boldsymbol{d}_2^{E,z} = S_-(\boldsymbol{k})\boldsymbol{z}\end{cases}$ $\begin{cases}\boldsymbol{d}_1^{E,xy} = \sqrt{2}S(\boldsymbol{k})\boldsymbol{x}_+\\ \boldsymbol{d}_2^{E,xy} = -\sqrt{2}S(\boldsymbol{k})\boldsymbol{x}_-\end{cases}$ $\begin{cases}\boldsymbol{d}_1^{E,\tilde{xy}} = \sqrt{2}S_-(\boldsymbol{k})\boldsymbol{x}_-\\ \boldsymbol{d}_2^{E,\tilde{xy}} = -\sqrt{2}S_+(\boldsymbol{k})\boldsymbol{x}_+\end{cases}$

3. Symmetry analysis and method

The point-group symmetry of monolayer H–*MXY* is C_{3v} and its basis gap functions are given in Table 1. Here we only consider the on-site and NN pairing channels. Depending on the spin angular momentum of the cooper pair, *i.e.*, spin-singlet ($S=0$) or spin-triplet ($S=1$), gap functions take the matrix form as:

$$\Delta_i^{\Gamma,\alpha}(\boldsymbol{k}) = \begin{cases} \Psi_i^{\Gamma,\alpha} \mathrm{i}\sigma_y, & \text{singlet pairing}, \\ \boldsymbol{d}_i^{\Gamma,\alpha} \cdot \boldsymbol{\sigma} \mathrm{i}\sigma_y, & \text{triplet pairing}, \end{cases} \tag{5}$$

where $\Psi_i^{\Gamma,\alpha}$ indicates the singlet pairing and $\boldsymbol{d}_i^{\Gamma,\alpha}$ is the $\boldsymbol{d}$ vector for the triplet pairing. Γ labels the different IR (do not be confused with the Γ point in the BZ) and α denotes the basis gap function belonging to it. Index $i=1,2$ is used to distinguish two equivalent gap functions in the same high dimensional IR, *e.g.*, E. Thus, the stable pairing in our model can be written as a linearized combination of these basis gap functions:

$$\Delta(\boldsymbol{k})/\Delta = \sum_{\Gamma,\alpha} c^{\Gamma,\alpha} \Delta^{\Gamma,\alpha}(\boldsymbol{k}), \tag{6}$$

where Δ is the gap size value and $c^{\Gamma,\alpha}$ denotes the relative amplitude of $\Delta^{\Gamma,\alpha}(\boldsymbol{k})$, with the normalization condition $\sum_{\Gamma,\alpha} |c^{\Gamma,\alpha}|^2 = 1$. From Table 1 we have four classes of $\boldsymbol{k}$-dependent basic gap structure: $C(\boldsymbol{k})$ for the extended s-wave pairing, $S(\boldsymbol{k})$ for the f-wave type, $C_\pm(\boldsymbol{k})$ and $S_\pm(\boldsymbol{k})$ denote the chiral $d\pm\mathrm{i}d$ and $p\mp\mathrm{i}p$-wave types, respectively. Distributions of these gap structures in the momentum space are shown in Fig. 2. From Figs. 2(a) and 2(b) one can see that there is a nodal loop around Γ point for the extended s-wave pairing and nodal lines along Γ–M directions for the f-wave. A pure s- or f-wave superconductor then could be a nodal superconductor. On the contrary, the $d+\mathrm{i}d$- and $p-\mathrm{i}p$-wave pairing gaps have finite nodes in the BZ and each node has its own chirality, as shown in Figs. 2(c) and 2(d). Here we define the chirality by computing the phase winding of the gap function along a counterclockwise loop around the node. It can be easily obtained from the plots that the winding numbers of these nodal points are $(w_\Gamma, w_{K(K')}) = (-2,1)$ for $d+\mathrm{i}d$ and $(w_\Gamma, w_{K(K')}, w_M) = (1,1,-1)$ for $p-\mathrm{i}p$. Obviously sum over the winding number of each node in the BZ gives zero. Superconductors of these two pairing forms are fully gapped and the winding number of superconducting gap on the FS is totally determined by the gap-function nodes enclosed by the FS sheets, which is also equivalent to the (first) Chern number.[46]

The intrinsic SOCs in our model destroy the inversion symmetry and give rise to admixture between singlet and triplet pairings. Lots of parity-mixed pairing states in the noncentrosymmetric superconductors have already been discussed in previous works.[52–57] Given that the $\boldsymbol{d}$ vector always tend to be paralleled to the SOC fields, *e.g.*, $\boldsymbol{g_k} = \boldsymbol{\alpha_k} + \boldsymbol{\beta_k}$ in our model, significant admixtures between ψ, $\boldsymbol{d}^{xy}$ and $\boldsymbol{d}^{z}$ are expected in a Janus monolayer with both strong in-plane Rashba ($\boldsymbol{\alpha_k}$) and out-of-plane Ising ($\boldsymbol{\beta_k}$) "magnetic fields".

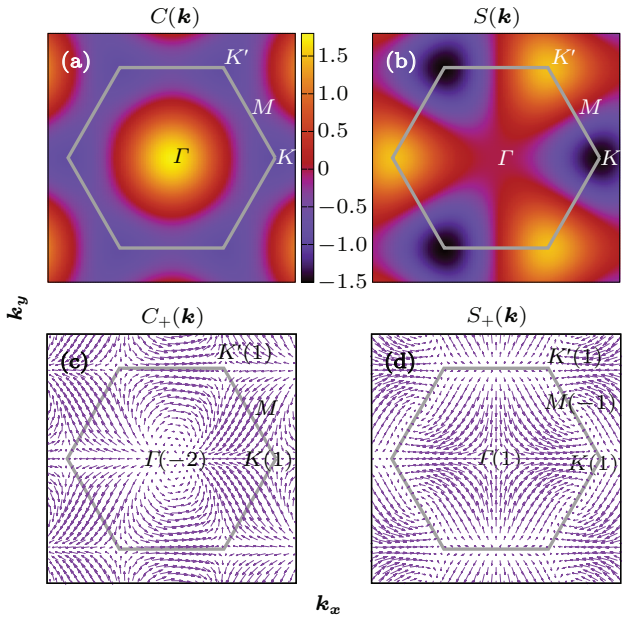


Fig. 2. Distribution of the gap structure (a) $C(\boldsymbol{k})$ [extended s-wave], (b) $S(\boldsymbol{k})$ [f-wave], (c) $C_+(\boldsymbol{k})$ [$d+\mathrm{i}d$-wave] and (d) $S_+(\boldsymbol{k})$ [$p-\mathrm{i}p$-wave] in the momentum space. The hexagonal BZ is indicated by the gray box. The bright and dark areas in panels (a), (b) represent positive and negative values. The length and angle of arrows in panels (c), (d) respectively give the amplitude and phase of the complex $C_+(\boldsymbol{k})$, $S_+(\boldsymbol{k})$. Winding numbers of each gap node are given in the brackets.

We obtain the T_c and the most favorable pairing $\Delta(\boldsymbol{k})$ by solving the linearized gap equation near T_c:

$$\begin{aligned} \Delta_{s_1 s_2}(\boldsymbol{k}) = T_c \sum_{\boldsymbol{k}' s_3 s_4 \omega_n} & V_{s_1 s_2 s_3 s_4}(\boldsymbol{k}, \boldsymbol{k}') \\ & \times [G(\boldsymbol{k}', \mathrm{i}\omega_n) \Delta(\boldsymbol{k}') G^t(-\boldsymbol{k}', \mathrm{i}\omega_n)]_{s_3 s_4}, \end{aligned} \tag{7}$$

where $G(\boldsymbol{k}', \mathrm{i}\omega_n)$ is the normal-state Matsubara Green's function, and $V(\boldsymbol{k}, \boldsymbol{k}')$ the pairing interaction with the spin index $s_j = \uparrow, \downarrow$. The form of $V(\boldsymbol{k}, \boldsymbol{k}')$ can be given by the basis gap functions as follows:

$$\begin{aligned} & V_{s_1 s_2 s_3 s_4}(\boldsymbol{k}, \boldsymbol{k}') \\ = & -v_0 \Psi^{A_1,on} \Psi^{*A_1,on} (\mathrm{i}\sigma_y)_{s_1 s_2} (\mathrm{i}\sigma_y)_{s_3 s_4} + \\ & -v_1 \sum_{\Gamma,i} \Psi_i^{\Gamma,nn} \Psi_i^{*\Gamma,nn} (\mathrm{i}\sigma_y)_{s_1 s_2} (\mathrm{i}\sigma_y)_{s_3 s_4} + \\ & -v_1 \sum_{\Gamma,\alpha,i} [\boldsymbol{d}_i^{\Gamma,\alpha} \cdot \boldsymbol{\sigma} \mathrm{i}\sigma_y]_{s_1 s_2} [\boldsymbol{d}_i^{\Gamma,\alpha} \cdot \boldsymbol{\sigma} \mathrm{i}\sigma_y]^*_{s_3 s_4}, \end{aligned} \tag{8}$$

where v_0, v_1 represent the on-site and NN pairing strengths respectively and the positive (negative) values of them denote attractive (repulsive) interactions.

4. Result and discussion

Our calculation allow us to construct an NN interaction-chemical potential superconducting phase diagram as shown

in Fig. 3. The conventional on-site s-wave is more stable than NN one only if when on-site interaction is stronger than the NN one ($v_1/v_0 < 1$), illustrated as bright blue regions in phase diagram. For the NN superconducting states in the rest of the phase diagram, the TRI $s+f+p$-wave pairing state (dark blue regions of the phase diagram), which corresponding to gap functions "$\Psi^{A_1,nn} + \boldsymbol{d}^{A_1,z} + \boldsymbol{d}^{A_1,xy}$", dominates the parameter space where $\mu > -0.08$ eV. By comparing to the monolayer MX_2, where A_1 phase is a nodal $s+f$-wave pairing state, we conclude that it is the large Rashba SOC of Janus structure that induces helical p-wave component $\boldsymbol{d}^{A_1,xy}$ in MXY. Typical relative amplitudes of the three pairing components are $(c^{A_1,nn}, c^{A_1,z}, c^{A_1,xy}) = (-0.24, 0.91, -0.34)$. The helical p-wave order parameter is stronger than the extended s-wave on the Γ-centered FS, leading to a full-gap $s+f+p$-wave state with a nontrivial topological invariant $\mathbb{Z}_2 = 1$. The $\mathbb{Z}_2$ number is calculated by using

$$\mathbb{Z}_2 = \frac{1}{2\pi i}\oint_C \mathrm{d}\boldsymbol{k}\cdot\nabla_{\boldsymbol{k}}\log[\mathrm{Pf}[A] + \mathrm{i}\delta], \tag{9}$$

$$A_{mn} = \langle m, \boldsymbol{k}|\Theta|n, \boldsymbol{k}\rangle \tag{10}$$

moded by 2 where $\mathrm{Pf}[A]$ is the Pfaffian of A. Θ is the time-reversal operator and $|n, \boldsymbol{k}\rangle$ is the eigenstate with an energy $E_{n,\boldsymbol{k}}$ of the superconducting Hamiltonian. C in Eq. (9) is the path enclosing half of the BZ, as shown in Ref. [58]. For topologically trivial (nontrivial) case, $\mathbb{Z}_2 = 0$ (1). Figure 4(a) displays the enlarged-energy spectrum of the $\mathbb{Z}_2 = 1$ topological phase, whose topologically protected Majorana helical edge states are highlighted by the red color.

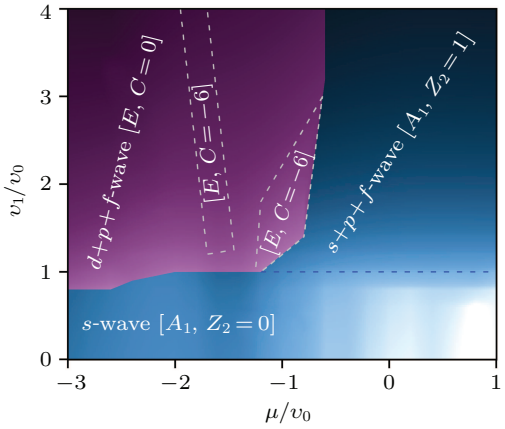


Fig. 3. Superconducting phase diagram of Janus monolayer MXY in the v_1–μ plane, with $v_0 = 0.1$ eV. The blue and purple denote the A_1 and E phases, respectively, and the dashed lines indicate the borders of topological phases. The critical temperature T_c exponentially increases from bright to dark, corresponding to a temperature range from 0 K to about 400 K. Topological invariant $C(i=1)$ or $\mathbb{Z}_2$ of each phase is also illustrated.

In addition, a $d+p+f$-wave pairing E phase, which is four-components and denoted by "$\Psi_i^{E,nn} + \boldsymbol{d}_i^{E,z} + \boldsymbol{d}_i^{E,xy} + \boldsymbol{d}_i^{E,\tilde{x}\tilde{y}}$", will be stabilized in the lower chemical potential regions (the purple regions in Fig. 3). In principle, two equivalent pairings in two dimensional IR respectively labeled by $i=1$ and $i=2$ could mix together in any ratios. However, this admixture could produce nodes in the superconducting gap, leading to a cost in the free energy of system. Based on the free-energy minimization, we conclude that the most stable pairing state below T_c should be a chiral state, either $i=1$ or $i=2$, rather than any combinations of them.[31,59] This indicates that the system will undergo a spontaneous time-reversal symmetry breaking when the temperature across the superconducting transition T_c. We choose $i=1$ for our following discussions. Besides the $d+\mathrm{i}d$- and $p-\mathrm{i}p$-wave pairings ($\Psi_1^{E,nn}$ and $\boldsymbol{d}_1^{E,z}$) in the $\uparrow\downarrow$ spin pairing channel, we also have $\boldsymbol{d}_1^{E,xy}$ which is an f-wave pairing emerging in the $\uparrow\uparrow$ channel and $\boldsymbol{d}_1^{E,\tilde{x}\tilde{y}}$ a $p-\mathrm{i}p$-wave pairing in $\downarrow\downarrow$ channel. Apart from counting the winding number of superconducting gap opened on the FS, one can also calculate the Chern number of this kind of full-gap nonunitary pairing through the equation

$$C = \frac{1}{2\pi}\sum_{E_n<0}\int_{\mathrm{BZ}}\mathrm{d}\boldsymbol{k}^2[\partial_{k_x}\mathcal{A}_{k_y}(n,\boldsymbol{k}) - \partial_{k_y}\mathcal{A}_{k_x}(n,\boldsymbol{k})], \tag{11}$$

where n denotes the occupied band of the BdG Hamiltonian $H_{\boldsymbol{k}}^{\mathrm{BdG}}$ and $\mathcal{A}_{k_j}(n,\boldsymbol{k}) = -\mathrm{i}\langle n,\boldsymbol{k}|\partial_{k_j}|n,\boldsymbol{k}\rangle$ is the adiabatic connection defined on it.

Our result shows that most of the E-phase regions in the diagram are topologically trivial, *i.e.*, $C=0$, except two islands with a Chern number $C=-6$ for $i=1$ ($C=6$ for $i=2$ owing to its opposite chirality), which are enclosed by the dashed gray lines in Fig. 3. These two islands are located nearby on both sides of the vHS (at $\mu/v_0 = -1.5$), indicating that the normal-state FS topology of Janus monolayer is not essential for the band topology of E-phase superconductivity. Typical values of the relative amplitudes of all basis gap functions in the trivial and nontrivial E phases are $(c_1^{E,nn}, c_1^{E,z}, c_1^{E,xy}, c_1^{E,\tilde{x}\tilde{y}}) = (0.87, -0.39, -0.12, -0.28)$ and $(0.8, -0.48, -0.14, -0.33)$, respectively. It is evident that a small modification of the ratios between these basis functions leads to a topological phase transition. More specifically, we attribute this topological nature difference to the Rashba-induced non-unitary $p+f$-wave components ($\boldsymbol{d}_1^{E,xy} + \boldsymbol{d}_1^{E,\tilde{x}\tilde{y}}$). The six Majorana chiral edge states corresponding to $C=-6$ phase is shown in Fig. 4(b). Here we remind the reader that this even-Chern-number topological superconductor does not support Majorana fermion modes in its topological defeats.[60] We also note that in the absence of Rashba splitting, the E-phase TRB $d+p$-wave pairing always be topologically trivial. This is due to the domination of $d+\mathrm{i}d$ component over $p-\mathrm{i}p$ component on the FS. Thus the topology of superconductivity is determined by the $d+\mathrm{i}d$ pairing, which gives a total winding number of zero on the three FS sheets of MX_2 as we discussed in Section 3.

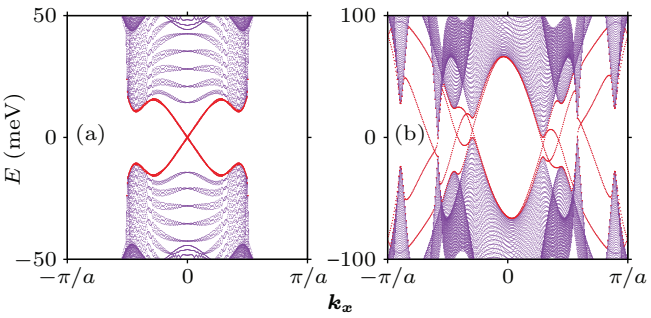


Fig. 4. Energy spectra of the topological (a) TRI $s+f+p$-wave ($A_1, \mathbb{Z}_2 = 1$) state, (b) TRB $d+p+f$-wave ($E, C = -6$) state of the Janus monolayer, with open-boundary conditions along y direction. Gap sizes are enlarged for sight and the gapless edge states are highlighted by the red.

5. Conclusions

In this paper, the possible forms of pairing in Janus monolayer TMDs with FS centered around both Γ and K (K') points have been investigated. Through analysis on the pairing symmetry and calculations based on the linearized gap equations, we have identified a $\mathbb{Z}_2$ topological $s+f+p$-wave superconducting state at the relatively high chemical potentials, and a chiral $d+p+f$-wave state with a large Chern number $|C| = 6$ when the chemical potential is lower. Unlike its parent MX_2 monolayers which are nodal or topologically trivial superconductors, our results show that Janus monolayer TMDs could be a promising candidate for the intrinsic helical and chiral TSCs.

Although we only focus on a specific model, the conclusions can be applied to all the superconducting Janus monolayer TMDs with strong-Rashba-splitting FS centered around Γ, *e.g.*, the group-V Janus H–*MXY* (M = Ta, Nb, *etc.*; X, Y = S, Se, *etc.*). There are superconducting conductance experiments observing zero bias conductance peak of the thin flakes of 2H–TaS_2 and 2H–$TaSe_2$ below T_c,[61,62] which indicates novel superconductivity in the atomic limit. Theoretical results suggest that these novel pairings could be $s+f$-wave and $d+p$-wave,[31,32,46] which both require a larger NN pairing attraction over on-site one in our framework. Consequently, it is most likely to realize the $s+f+p$-wave and $d+p+f$-wave topological states in Janus monolayer of group-V TMDs if the same assumption is taken for this family of materials.

Acknowledgements

We acknowledge Wei-Jian Li for useful discussions. Xian-Dong Li also thanks Ai-Lei He for helpful suggestions. Project supported by the National Natural Science Foundation of China (Grant No. 11904155).

References

[1] Fu L and Kane C L 2008 *Phys. Rev. Lett.* **100** 096407
[2] Schnyder A P, Ryu S, Furusaki A and Ludwig A W W 2008 *Phys. Rev. B* **78** 195125
[3] Kitaev A 2009 *AIP Conf. Proc.* **1134** 22
[4] Fu L and Berg E 2010 *Phys. Rev. Lett.* **105** 097001
[5] Ryu S, Schnyder A P, Furusaki A and Ludwig A W W 2010 *New J. Phys.* **12** 065010
[6] Qi X L and Zhang S C 2011 *Rev. Mod. Phys.* **83** 1057
[7] Das A, Ronen Y, Most Y, Oreg Y, Heiblum M and Shtrikman H 2012 *Nat. Phys.* **8** 887
[8] Fidkowski L, Chen X and Vishwanath A 2013 *Phys. Rev. X* **3** 041016
[9] Sato M and Ando Y 2017 *Rep. Prog. Phys.* **80** 076501
[10] Rice T M and Sigrist M 1995 *J. Phys.: Condens. Matter* **7** L643
[11] Baskaran G 1996 *Physica B* (Amsterdam) **223** 490
[12] Nelson K D, Mao Z Q, Maeno Y and Liu Y 2004 *Science* **306** 1151
[13] Huang W 2021 *Chin. Phys. B* **30** 107403
[14] Stewart G R 1984 *Rev. Mod. Phys.* **56** 755
[15] Varma C M 1985 *Phys. Rev. Lett.* **55** 2723
[16] De Visser A, Menovsky A and Franse J 1987 *Phys. B+C* (Amsterdam) **147** 81
[17] Sato M, Takahashi Y and Fujimoto S 2009 *Phys. Rev. Lett.* **103** 020401
[18] Sau J D, Lutchyn R M, Tewari S and Das Sarma S 2010 *Phys. Rev. Lett.* **104** 040502
[19] Clayman B and Frindt R 1971 *Solid State Commun.* **9** 1881
[20] Boaknin E, Tanatar M A, Paglione J, Hawthorn D, Ronning F, Hill R W, Sutherland M, Taillefer L, Sonier J, Hayden S M and Brill J W 2003 *Phys. Rev. Lett.* **90** 117003
[21] Huang C L, Lin J Y, Chang Y T, Sun C P, Shen H Y, Chou C C, Berger H, Lee T K and Yang H D 2007 *Phys. Rev. B* **76** 212504
[22] Berthier C, Molinie P and Jerome D 1976 *Solid State Commun.* **18** 1393
[23] Mutka H 1983 *Phys. Rev. B* **28** 2855
[24] Castro Neto A H 2001 *Phys. Rev. Lett.* **86** 4382
[25] Lu J M, Zheliuk O, Leermakers I, Yuan N F Y, Zeitler U, Law T and Ye J T 2015 *Science* **350** 1353
[26] Xi X, Wang Z, Zhao W, Park J H, Tuen Law K, Berger H, Forro L, Shan J and Mak K 2015 *Nat. Phys.* **12** 139
[27] Saito Y, Nakamura Y, Bahramy M S, Kohama Y, Ye J, Kasahara Y, Nakagawa Y, Onga M, Tokunaga M, Nojima T, *et al.* 2016 *Nat. Phys.* **12** 144
[28] Xing Y, Zhao K, Shan P, Zheng F, Zhang Y, Fu H, Liu Y, Tian M, Xi C, Liu H, Feng J, Lin X, Ji S, Chen X, Xue Q K and Wang J 2017 *Nano Lett.* **17** 6802
[29] Lu J, Zheliuk O, Chen Q, Leermakers I, Hussey N E, Zeitler U and Ye J 2018 *Proc. Natl. Acad. Sci. USA* **115** 3551
[30] Barrera S C, Sinko M R, Gopalan D P, Sivadas N, Seyler K L, Watanabe K, Taniguchi T, Tsen A W, Xu X, Xiao D, *et al.* 2018 *Nat. Commun.* **9** 1427
[31] Yuan N F Q, Mak K F and Law K T 2014 *Phys. Rev. Lett.* **113** 097001
[32] Hsu Y T, Vaezi A, Fischer M H and Kim E A 2017 *Nat. Commun.* **8** 14985
[33] Lu A Y, Zhu H, Xiao J, Chuu C P, Han Y, Chiu M H, Cheng C C, Yang C W, Wei K H, Yang Y, *et al.* 2017 *Nat. Nanotechnol.* **12** 744
[34] Zhang J, Jia S, Kholmanov I, Dong L, Er D, Chen W, Guo H, Jin Z, Shenoy V B, Shi L, *et al.* 2017 *ACS Nano* **11** 8192
[35] Li R, Cheng Y and Huang W 2018 *Small* **14** 1802091
[36] Hu T, Jia F, Zhao G, Wu J, Stroppa A and Ren W 2018 *Phys. Rev. B* **97** 235404
[37] Shi W and Wang Z 2018 *J. Phys.: Condens. Matter* **30** 215301
[38] He J and Li S 2018 *Comput. Mater. Sci.* **152** 151
[39] Zhou W, Chen J, Yang Z, Liu J and Ouyang F 2019 *Phys. Rev. B* **99** 075160
[40] Yagmurcukardes M, Sevik C and Peeters F M 2019 *Phys. Rev. B* **100** 045415
[41] Zhang K, Guo Y, Ji Q, Lu A Y, Su C, Wang H, Puretzky A A, Geohegan D B, Qian X, Fang S, *et al.* 2020 *J. Am. Chem. Soc.* **142** 17499
[42] Mikkelsen A E, Bolle F T, Thygesen K S, Vegge T and Castelli I E 2021 *Phys. Rev. Mater.* **5** 014002
[43] Petri. M M, Kremser M, Barbone M, Qin Y, Sayyad Y, Shen Y, Tongay S, Finley J J, Botello-Mendez A R and Muller K 2021 *Phys. Rev. B* **103** 035414
[44] Zheng T, Lin Y C, Yu Y, Valencia-Acuna P, Puretzky A A, Torsi R, Liu C, Ivanov I N, Duscher G, Geohegan D B, *et al.* 2021 *Nano. Lett.* **21** 931
[45] Sanders C E, Dendzik M, Ngankeu A S, Eich A, Bruix A, Bianchi M, Miwa J A, Hammer B, Khajetoorians A A and Hofmann P 2016 *Phys. Rev. B* **94** 081404
[46] Chen W, Zhu Q, Zhou Y and An J 2019 *Phys. Rev. B* **100** 054503

[47] Navarro-Moratalla E, Island J, Manas-Valero S, Pinilla-Cienfuegos E, Castellanos-Gomez A, Quereda J, Rubio-Bollinger G, Chirolli L, Silva-Guillen J, Agrait N, *et al.* 2016 *Nat. Commun.* **7** 11043

[48] Zhao J, Wijayaratne K, Butler A, Yang J, Malliakas C D, Chung D Y, Louca D, Kanatzidis M G, van Wezel J and Chatterjee U 2017 *Phys. Rev. B* **96** 125103

[49] Rossnagel K, Rotenberg E, Koh H, Smith N V and Kipp L 2005 *Phys. Rev. B* **72** 121103

[50] Ge Y and Liu A Y 2012 *Phys. Rev. B* **86** 104101

[51] Yan J A, Cruz M A D, Cook B and Varga K 2015 *Sci. Rep.* **5** 16646

[52] Sato M and Fujimoto S 2009 *Phys. Rev. B* **79** 094504

[53] Tanaka Y, Mizuno Y, Yokoyama T, Yada K and Sato M 2010 *Phys. Rev. Lett.* **105** 097002

[54] Goryo J, Fischer M H and Sigrist M 2012 *Phys. Rev. B* **86** 100507

[55] Youn S J, Fischer M H, Rhim S H, Sigrist M and Agterberg D F 2012 *Phys. Rev. B* **85** 220505

[56] Schnyder A P, Brydon P M R and Timm C 2012 *Phys. Rev. B* **85** 024522

[57] Yip S 2014 *Annu. Rev. Condens. Matter Phys.* **5** 15

[58] Kane C L and Mele E J 2005 *Phys. Rev. Lett.* **95** 146802

[59] Sigrist M and Ueda K 1991 *Rev. Mod. Phys.* **63** 239

[60] Sato M, Takahashi Y and Fujimoto S 2010 *Phys. Rev. B* **82** 134521

[61] Galvis J A, Rodiere P, Guillamon I, Osorio M R, Rodrigo J G, Cario L, Navarro-Moratalla E, Coronado E, Vieira S and Suderow H 2013 *Phys. Rev. B* **87** 094502

[62] Galvis J A, Chirolli L, Guillamon I, Vieira S, Navarro-Moratalla E, Coronado E, Suderow H and Guinea F 2014 *Phys. Rev. B* **89** 224512